



Fingerprinting-assisted UWB-based localization technique for complex indoor environments

Sandra Djosic ^{*}, Igor Stojanovic, Milica Jovanovic, Tatjana Nikolic, Goran Lj. Djordjevic

University of Nis, Faculty of Electronic Engineering, Aleksandra Medvedeva 14, 18000 Nis, Serbia



ARTICLE INFO

Keywords:
Indoor localization
Ultra-wideband
Fingerprinting
Trilateration
Machine learning

ABSTRACT

Among the numerous radio-based solutions for indoor localization, ultra-wideband (UWB) technology is of particular interest due to its signal characteristics. The wide bandwidth of the UWB signal provides a fine time resolution of the transmitted pulses that enables a centimetre-level ranging accuracy under line-of-sight (LOS) conditions even in multipath intensive indoor environments. Nevertheless, it is still a challenge to implement accurate UWB-based localization in complex multi-room indoor environments at low cost because of a large number of static UWB anchors that may need to be deployed in order to provide an adequate LOS coverage in every segment of the environment. Therefore, there is a strong interest in developing UWB-based localization techniques that will provide acceptable accuracy under partially LOS coverage conditions. In this paper, we present a novel hybrid method that combines two conventional localization techniques, trilateration and fingerprinting, to address the problem of cost-effective UWB-based localization in complex indoor environments. With the proposed method, the target location is determined by a trilateration algorithm, while a fingerprinting-based algorithm is used to provide additional distances for trilateration in cases when there is an insufficient number of available LOS measurements. The additional distances are generated by a non-parametric regression algorithm that relies on a fingerprint database to map all available online range measurements (LOS as well non-LOS) to distances between the target and the set of pre-defined reference points. To minimize human effort in fingerprint collection, the indoor environment is site-surveyed in a room-by-room fashion with auxiliary UWB anchors temporarily placed at up to three reference points in the surveyed room. The method is validated through an extensive indoor measurement campaign with commercially available UWB transceivers. The experimental results show that the proposed method achieves sub-decimetre level localization accuracy under typical real-world conditions.

1. Introduction

The task of an indoor localization system (ILS) is to determine and track the location of a person or an object in a closed indoor environment. In recent years, ILSs have attracted considerable research interest due to their potential to significantly impact everyday life in the near future. Application areas include health, industry, disaster management, building management, surveillance, and many more (Zafari et al., 2019; Bergeron, Bouchard, Gaboury, & Giroux, 2018). Of particular interest are radio signal-based ILSs, e.g., Wi-Fi, Bluetooth low energy (BLE), and ultra-wideband (UWB), because radio transceivers are built at small form factors with low power consumption, and can be integrated into existing devices (Belmonte-Fernandez, Montoliu, Torres-Sospedra,

Sansano-Sansano, & Chia-Aguilar, 2018; Davidson & Piché, 2016; Farid, Nordin, & Ismail, 2013; Velimirovic, Djordjevic, Velimirovic, & Jovanovic, 2012). Such systems typically consist of a set of anchor nodes (ANs), placed at fixed locations in the area of interest, and a target node (TN) carried by the person or attached to the object that needs to be localized. The location of the TN is estimated by a localization algorithm, which interprets some physical parameters obtained from received radio signals (Liu, Darabi, Banerjee, & Liu, 2007). However, despite many localization technologies and techniques available today, the design and deployment of radio signal-based ILS is still a challenging task, especially in indoor environments of complex geometry (multiple rooms, rooms of irregular shapes, doors, corridors, presence of obstacles, etc.), which are characterized by radio signal attenuation, presence of

* Corresponding author.

E-mail addresses: sandra.djosic@elfak.ni.ac.rs (S. Djosic), igor.stojanovic@elfak.ni.ac.rs (I. Stojanovic), milica.jovanovic@elfak.ni.ac.rs (M. Jovanovic), tatjana.nikolic@elfak.ni.ac.rs (T. Nikolic), goran.lj.djordjevic@elfak.ni.ac.rs (G.Lj. Djordjevic).

different interfering signals, and harsh multipath conditions (Kaemarungsi & Krishnamurthy, 2012).

Nowadays, UWB is considered the most promising radio-based ILS technology for harsh environments and accuracy-critical applications (Alarifi et al., 2016; Ruiz & Granja, 2017; Tiemann, Schweikowski, & Wietfeld, 2015). The most important characteristic of the UWB radio technology is the large bandwidth in comparison with prevalent narrowband systems (e.g., Wi-Fi, and BLE). One result of the large bandwidth is that due to the inverse relation between the time of flight (TOF) estimation error and signal bandwidth, the distance between two UWB devices can be measured with centimetre-level accuracy, even in multipath intensive indoor environments (Zwirello et al., 2014; Zhang, Orlik, Sahinoglu, Molisch, & Kinney, 2009). With accurate distance information to at least three ANs at disposal, the location of the TN can be estimated with a sub-decimetre level accuracy by applying standard trilateration techniques. Note that the high localization accuracy is essential for many ILS applications such as precise target tracking, and manoeuvring of a robot in tight spaces (e.g., when passing through a doorway). Because of large bandwidth, UWB is also resilient to multipath interference and fading and can pass through obstacles and penetrate walls in buildings, thus enabling non-line-of-sight (NLOS) communication and ranging. However, high localization accuracy is attainable only under the LOS operating conditions. With the absence of the LOS path, the transmitted signal could only reach the receiver through penetrated, reflected, diffracted, or scattered paths, called NLOS paths. Signals propagating in NLOS conditions are usually delayed and attenuated, which introduces a positive bias in TOF-based ranging and can significantly degrade the performance of the UWB localization system (Ferreira, Fernandes, Catarino, & Monteiro, 2017).

In general, there are two approaches to how UWB localization is applied in complex multi-room indoor environments. The first one is the deployment of a sufficiently large number of ANs in order to provide LOS paths to at least three ANs in every part of the indoor environment. At the run-time, the localization system identifies and discards NLOS measurements, and uses only LOS measurements for location estimation (Gururaj, Rajendra, Song, Law, & Cai, 2017; You, Li, Zhao, & Gao, 2015). By using only LOS measurements, this full LOS coverage deployment strategy ensures consistently high localization accuracy over the entire coverage area, but it may incur a high system cost in indoor environments of complex geometry (e.g. houses or office buildings with many rooms and/or rooms with irregular shapes). Therefore, in this paper, our focus is on the second approach, which relies on a partial LOS coverage deployment strategy to trade-off localization accuracy for a significant saving in system cost. With the partial LOS coverage, a simple identify-and-discard approach of handling NLOS measurements is not adequate because the removal of NLOS measurements may leave the localization system with an insufficient number of distance measurements to perform spatial localization. Instead, all available measurements (LOS as well as NLOS) should be used for location estimation. One approach is to first identify NLOS measurements, and then employ a suitable error mitigation technique to improve the accuracy of NLOS ranges before being used by a localization algorithm (Garcia, Poudereux, Hernandez, Urena, & Gualda, 2015; Khodjaev, Park, & Malik, 2010). The location fingerprinting is another widely adopted data-driven technique for UWB localization under mixed LOS/NLOS conditions, which usually involves two phases. The offline training phase consists of building a fingerprint database with location signatures, also called fingerprints, based on location-dependent received signal parameters (e.g., signal time-of-flight, channel impulse response (CIR), and received signal strength (RSS)), which are collected at a number of locations in the area of interest. Then, in the online phase, any observed fingerprint is compared against the ones stored in the fingerprint database to infer the location of the TN. The major advantage of the fingerprinting-based methods is that they can provide accurate location estimations in the challenging multipath environments without requiring the existence of LOS paths between the TN and ANs, nor an

analytical characterization of the relation between the signal parameters and the TN's location. However, the task of building the fingerprint database is usually very labour-intensive and time-consuming, involving substantial human efforts in providing accurate ground truth location information for each collected fingerprint. Moreover, the fingerprint database should be updated timely to reflect environmental changes, which may incur a high maintenance cost.

In this paper, we propose a practical and cost-effective fingerprinting-assisted UWB-based localization (FAUL) method, which offers high accuracy in multi-room indoor environments with a reduced number of ANs. The primary goal of the proposed method is to provide a near LOS localization accuracy in partially LOS covered indoor scenarios. To this end, FAUL employs a hybrid localization scheme, which combines a trilateration algorithm with location fingerprinting. The TN location is determined by a weighted trilateration algorithm, while a fingerprinting-based algorithm is used to provide additional distances for trilateration in cases when less than three TN-to-AN LOS measurements are available. FAUL distinguishes from traditional fingerprinting-based approaches in that it uses different anchor configurations during the offline and online phases. During the offline phase, a set of permanently-installed ANs is temporarily extended with a set of auxiliary ANs that are strategically distributed throughout the surveying-area to form a full LOS coverage configuration. With such a setup, the fingerprint database is built by only taking UWB-measured TN-to-AN distances, avoiding the need for manual labelling individual fingerprints with ground truth coordinates. In this manner, a large indoor area can be site-surveyed automatically in a relatively short amount of time, producing a dense fingerprint database. In the online phase, when only permanent ANs are present, the fingerprint database is used to predict distances between TN and the points where auxiliary ANs were placed during the offline phase. The predicted distances are then used as additional distances for trilateration when needed.

The real-world data used in this paper were collected in a measurement campaign that was carried out in a multi-room residential apartment. In the experiments, we used six permanent UWB anchors distributed throughout the five rooms to explore how the FAUL localization performance depends on fingerprint density and the number of available LOS measurements. The results validate our overall localization strategy and demonstrate that the FAUL method can achieve sub-decimetre level localization accuracy under typical real-world conditions allowing significant saving in the number of deployed ANs.

The remainder of this paper is structured as follows: In Section 2, we summarize related studies on radio signal-based indoor localization. The proposed algorithm is presented in Section 3. We start with the localization setup, anchor deployment strategy, and an outline of the underlying ranging protocol. Then, we present detailed descriptions of the offline training and online localization phases of the proposed localization method. The experimental results are presented in Sections 4 and 5 provides conclusions.

2. Related works

The last decade has witnessed tremendous efforts at building small, medium, and large-scale ILSs using various radio signal-based technologies, especially using Wi-Fi, and more recently BLE and UWB (Gu, Lo, & Niemegeers, 2009; Liu, Darabi, Banerjee, & Liu, 2007). The following two general localization strategies are commonly used for designing ILSs: *i*) the range-based localization, which assumes the existence of a ranging mechanism relating distance to observed signal parameters, and *ii*) the fingerprinting-based localization, which relates an observed set of signal parameters to ones at known locations. As narrowband communication and multipath propagation make precise ranging extremely challenging in indoor environments, most Wi-Fi ILSs follow the fingerprinting approach, usually based on RSS signal vectors (Bahl & Padmanabhan, 2000; Huang, He, & Du, 2019; Stella, Russo, & Begović, 2014). Significant research has been devoted to the online phase, aiming

to improve the localization accuracy using either deterministic or probabilistic algorithms to match the online fingerprint with those in the fingerprint database (He & Chan, 2015). With deterministic algorithms, the TN is located at the closest fingerprint location in the RSS space, using a suitable similarity metric for fingerprint comparison (e.g., Euclidean distance, and cosine similarity). Deterministic methods can be implemented using a variety of machine learning algorithms, e.g., k-nearest neighbours (kNN) (Bahl & Padmanabhan, 2000), the support vector machine (Cai, Rai, & Yu, 2015), and the decision trees (Banitaan, Azzeh, & Nassif, 2016), with usually low computational complexity. With probabilistic algorithms, RSS values are represented as a probability distribution, and the algorithm calculates the probability of a TN's location based on the online measurements and fingerprint database (Sciarrone et al., 2016; Zhao, Huang, & Wang, 2019). Probabilistic techniques are computationally more expensive than deterministic techniques but provide higher accuracy and robustness to missing or incomplete data (Bisio, Lavagetto, Marchese, & Sciarrone, 2013).

The main advantages of the UWB radio technology are the high temporal resolution, and the capacity of resolving individual multipath components, which enables accurate indoor ranging. Therefore, the UWB-based ILSSs usually employ range-based localization techniques, especially in small-scale systems where full LOS coverage can easily be attained with a small number of deployed ANs. The range-based methods also involve two phases. In the ranging phase, TN-to-ANs distances are estimated based on time delay information of the received radio signal, which is typically made available by UWB hardware (DecaWave, 2018). In the localization phase, with a sufficient number of distance estimates at disposal, a trilateration or multilateration algorithm is used to compute the TN's location (Yan, Tiberius, Janssen, Teunissen, & Bellusci, 2013). However, reaching a high localization accuracy under predominantly NLOS conditions in complex large-scale indoor environments requires more elaborate methods, which often involves fingerprinting. To cope with the presence of NLOS induced ranging errors, the TN's location can be estimated using the conventional fingerprinting approach (Luo & Gao, 2016; Steiner & Wittneben, 2009; Yu, Laaraiedh, Avrillon, & Uguen, 2011), or a fingerprinting scheme can be integrated within a range-based technique for identifying NLOS measurements (Caso, Le, De Nardis, & Di Benedetto, 2018), and/or estimating the NLOS ranging errors (Guvenc, Chong, & Watanabe, 2007; Güvenç, Chong, Watanabe, & Inamura, 2007). Instead of RSS measurements, UWB fingerprints typically include either range estimates (Bogdani, Vouyioukas, & Nomikos, 2016; Song, Zhang, Long, & Hu, 2017) or multiple location-dependent features extracted from the channel impulse response (CIR) (Dardari, Conti, Ferner, Giorgetti, & Win, 2009; Luo & Gao, 2016). The CIR-based UWB fingerprinting improves localization accuracy at the expense of the increased size of the fingerprinting database.

The main challenge in both Wi-Fi and UWB fingerprinting methods is the construction of a fingerprinting database, which can be time and cost-prohibitive for large-scale environments if the ground truth coordinates are determined manually. The problem is particularly severe in the case of UWB-based localization, in which a dense fingerprint database is essential to achieve the high expected localization accuracy. Several methods have been proposed to reduce the site-survey effort. An approach is to reduce the number of survey points, and then apply interpolation and extrapolation methods to recover missing fingerprint data (Chai & Yang, 2007; Talvitie, Renfors, & Lohan, 2015). Methods for fingerprint database construction by unsupervised learning and crowdsourcing have also been proposed (Chintalapudi, Padmanabha, & Padmanabhan, 2010; Yang, Wu, & Liu, 2012). However, by trading-off the localization accuracy for survey cost, these methods are often insufficient for applications with high accuracy requirements. In (Prorok & Martinoli, 2014), offline fingerprints are collected by a mobile robot equipped with a UWB tag. During the training phase, fingerprints are labelled with ground truth coordinates obtained by accurately tracking the robot position with an overhead camera system. Although this

approach allows for the fast construction of a high-density fingerprint database, its practicality is limited by the cost of the external high-precision reference localization system.

The UWB-based localization strategy we propose in this work follows the general fingerprinting-based approach, as it relies on the offline fingerprint measurements to improve the localization accuracy during the online phase. One of the unique features of the proposed method is that it offers a simple solution for improving the productivity of the training phase. Our proposed FAUL method avoids manual labelling of the offline fingerprints with ground truth coordinates by using a few auxiliary UWB ANs, rather than deploying a costly full-featured external localization system as in Prorok and Martinoli (2014). Another unique feature of the proposed FAUL method relates to how the fingerprint database is used in the online phase. Different from other fingerprinting-based approaches, FAUL utilizes the fingerprint database to predict the ranging responses of the auxiliary ANs, and then uses the predicted ranges for trilateration whenever less than three LOS distance measurements are available. In this study, we are also focused on investigating the accuracy implication of using auxiliary UWB ANs for system training. To avoid biasing the results with the impact of advanced fingerprinting-related implementation options (e.g. probabilistic fingerprinting, the use of CIR parameters, and advanced machine learning algorithms), we chose to adopt a deterministic kNN-based fingerprinting scheme, in which the UWB-measured distances are used as location signatures.

3. Fingerprinting-assisted UWB-based indoor localization

3.1. Localization setup

The proposed FAUL indoor localization scheme addresses the mobile TN localization problem in multi-room indoor environments using UWB-enabled devices. Although it can be adapted to numerous application scenarios, in this paper we present the FAUL localization scheme within the context of a system for real-time 2D localization of an autonomous domestic service robot. We assume a single robot operating within a typical multi-room residential apartment. The FAUL infrastructure includes: *a*) a set of anchor placeholders, *b*) a set of ANs, *c*) single TN, and *d*) a location server. Anchor placeholders (APs) are installed at fixed and known positions in the apartment, and each placeholder is assigned a unique identifier (ID) in the range $[0, n-1]$, where n is the number of placeholders deployed. ANs are designed to be easily inserted into and removed from APs. ANs do not have pre-assigned IDs, but each AN takes over the ID of the AP in which it is inserted. The TN is attached to the robot and periodically performs UWB ranging to all ANs. The measured distances are collected by the TN and then sent to the location server, which executes the localization algorithm to obtain the estimated location of the TN.

3.2. Anchor deployment

FAUL requires a specific AP deployment strategy in order to achieve acceptable localization accuracy at minimum cost. Fig. 1 shows an exemplary deployment of APs within a five-room apartment. There are two types of APs, represented by red-filled and white boxes. The *primary* APs (red boxes) are dedicated to permanent ANs, i.e. those ANs that remain permanently inserted into their placeholders, except in a case of failure or system reconfiguration. The *secondary* APs (white boxes) are for auxiliary ANs, which are used during the offline training phase, only.

The APs are deployed in two steps. In the first step, the user defines locations of primary APs. FAUL requires that each point in the localization space is covered by at least three permanent ANs. A point is covered by an AN if the successful (LOS or NLOS) ranging between the AN and TN located at that point can be performed with a high probability. Because the UWB signal can penetrate walls, one primary AP per room is usually sufficient to provide the required permanent AN

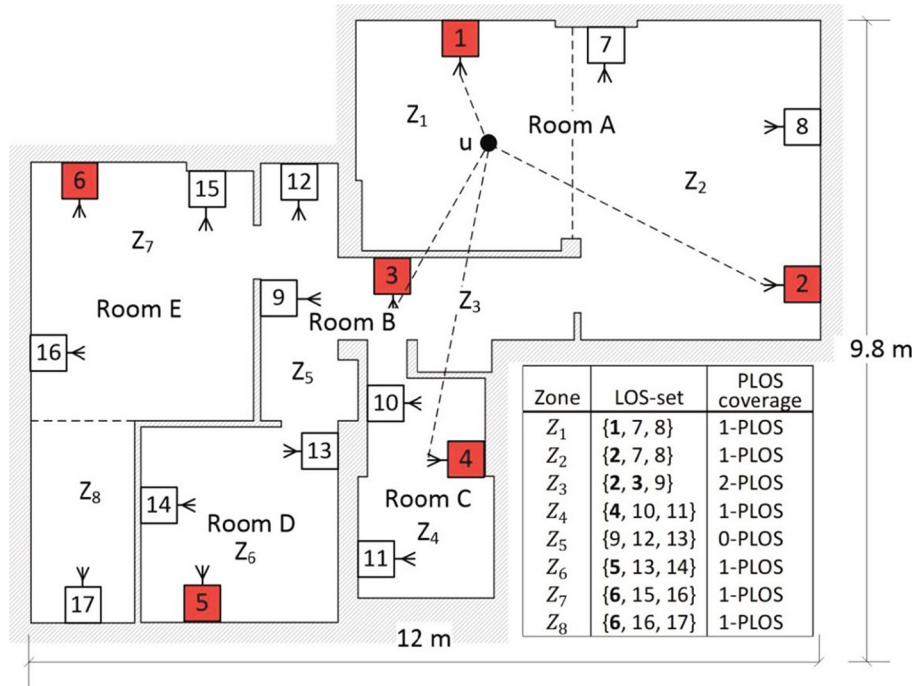


Fig. 1. The map of experimental environment. Red boxes denote primary, while white boxes denote secondary anchor placeholders.

coverage in a typical deployment scenario. For example, point u in Fig. 1 is covered by four permanent ANs: 1, 2, 3, and 4. It is LOS-covered by ANs 1 and 2, and NLOS-covered by ANs 3 and 4. The remaining two ANs, 5 and 6, are too far or obstructed by several walls preventing reliable ranging with a TN located at point u .

In the second deployment step, the user adds secondary APs in order to improve LOS coverage to the level required for the offline training. The locations of secondary APs are chosen in a way so that each point in the localization space is LOS-covered by at least three primary/secondary APs. To this end, the user first divides the localization space into zones. Typically, a zone corresponds to a room, although the rooms with irregular shapes can be subdivided into two or more smaller zones. Then, the user adds and arranges secondary APs so that all points in the same zone are LOS-covered by the same set of three primary/secondary APs. The set of three APs that provide LOS coverage in a zone is referred to as LOS-set of that zone. The LOS-sets do not have to be mutually disjoint, i.e., the same AP can provide LOS coverage in more than one neighbouring zones. We say that a zone is p -PLOS covered if among three APs that provide LOS coverage in the zone there are p primary APs (and $3-p$ secondary APs). After the deployment phase, the deployment-related parameters are stored in the configuration database. These parameters include: a) information about APs, their roles (primary or secondary) and locations within the environment, and b) LOS-sets of all zones.

For example, each room in Fig. 1, except rooms A and E, constitutes a zone, whereas rooms A and E are divided into two zones each. Note that only two secondary APs are sufficient to provide LOS coverage in both zones of room A. APs 7 and 8 together with primary AP 1 form LOS-set of zone Z_1 , while the same two secondary APs and primary AP 2 form LOS-set of zone Z_2 . LOS-sets of all zones are listed in the table in Fig. 1. Identifiers of primary APs in LOS-sets are written in bold. As can be noticed, zone Z_3 is the only zone with 2-PLOS coverage in this deployment. The LOS-set of zone Z_5 includes secondary APs, only. The remaining zones are 1-PLOS covered. There is no 3-PLOS covered zone in this deployment.

3.3. Ranging protocol

The distance between two UWB radio transceivers is commonly estimated by carrying out the alternative double-sided two-way ranging (AltDS-TWR) method (Neirynck, Luk, & McLaughlin, 2016). As shown in Fig. 2, AltDS-TWR is a TOF based method, which requires exchanging of three messages (*Poll*, *Response*, and *Final*) between an initiator (node A) and a responder (node B). During the message exchange, nodes A and B take timestamps (t_1, \dots, t_6) of receive and send events on the physical layer using their respective local clocks. The timestamps are then used to calculate the time of flight, and therefore the distance between nodes A and B. The time of flight (T_{tof}) is calculated by substituting measured round-trip times ($T_{\text{round1}}, T_{\text{round2}}$) and reply times ($T_{\text{replyA}}, T_{\text{replyB}}$) into the formula (1). Note that the distance is calculated by the responder node B after it receives T_{round1} and T_{replyA} from the initiator node A.

$$T_{\text{tof}} = \frac{T_{\text{round1}} T_{\text{round2}} - T_{\text{replyA}} T_{\text{replyB}}}{T_{\text{round1}} + T_{\text{round2}} + T_{\text{replyA}} + T_{\text{replyB}}} \quad (1)$$

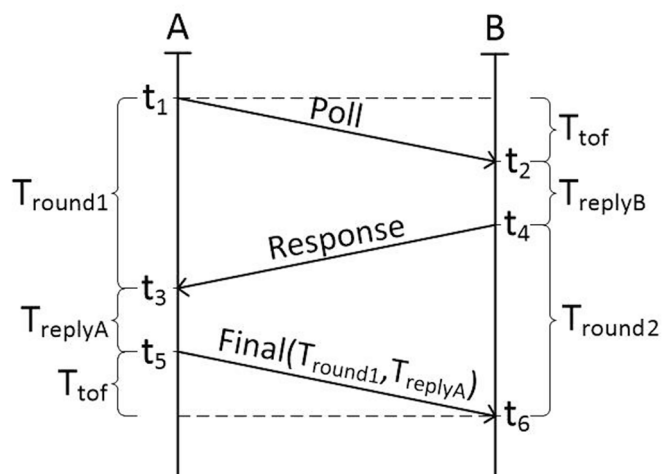


Fig. 2. Asymmetric double-sided two-way ranging method.

In FAUL, distances between the TN and ANs are obtained through periodic ranging rounds, where each round involves performing AltDS-TWR ranging between the TN and all ANs in succession. During the ranging round, the TN calculates and stores distances into the distance vector \mathbf{d} . The distance vector consists of n elements, and element d_i contains the measured distance between the TN and i th AN, that is, the AN inserted into the AP assigned with an ID value of i . If any AN is either not available or the ranging with the AN was not successful, then the corresponding element of vector \mathbf{d} is set to 0. A ranging round is considered successful if, at the end of the round, the distance vector contains at least three non-zero distance values. In the case of the unsuccessful ranging round, the distance vector is discarded by the TN. Otherwise, the TN sends the distance vector to the location server for further processing.

3.4. Offline training phase

FAUL requires an offline training phase for building fingerprint databases. It is assumed that the permanent ANs are already inserted in the corresponding primary APs. Additionally, the user should have at his/her disposal three auxiliary ANs to use during the training phase. The fingerprints are collected zone-by-zone. Before starting surveying a zone, auxiliary ANs are inserted into all secondary APs that are included in the LOS-set of that zone. During the zone survey, the location server is put in an automatic fingerprint collection mode wherein the ranging rounds are initiated periodically. The distance vectors are collected while the robot is scanning the area of the zone (e.g. by moving in a rectangular path). The only requirement is that the robot visits all parts of the zone. After the zone is surveyed, the auxiliary ANs are moved to the next zone, and the process is repeated. Note that the use of auxiliary ANs during the zone survey ensures that each collected distance vector will contain at least three LOS measured distances, which should compensate for the lack of ground truth coordinates of the TN's location.

Based on each distance vector \mathbf{d} received from the TN during the training phase, the location server creates two fingerprints for inserting into two separate fingerprint databases: the *distance database*, and the *zone database* (Fig. 3). The fingerprints in both databases are labelled with the zone ID and differ in the location-dependent parameter extracted from the distance vector. The fingerprint for distance database contains a complete distance vector, i.e. it is defined as a pair of $f_d = (zid, \mathbf{d})$, where zid is the zone ID. The fingerprint for the zone database is a pair of $f_z = (zid, \mathbf{c})$, where $\mathbf{c} = [x, y]^T$ is the 2D coarse position of the fingerprint, which is calculated through the least square-based multilateration algorithm by using measured distances to permanent ANs,

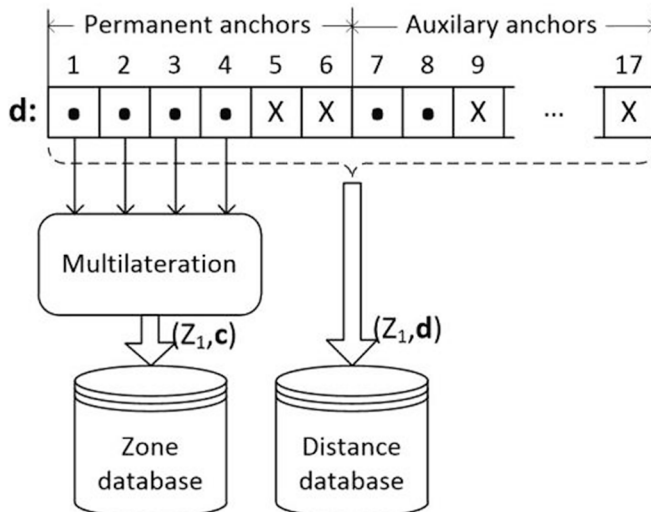


Fig. 3. Fingerprint databases construction procedure.

only. The least-square multilateration algorithm finds fingerprint's coarse coordinates $\mathbf{c} = [x, y]^T$ that satisfy the following minimization problem:

$$\hat{\mathbf{c}} = [\hat{x}, \hat{y}]^T = \underset{x,y}{\operatorname{argmin}} \sum_{i \in S} (\|\mathbf{a}_i - \mathbf{c}\| - d_i)^2 \quad (2)$$

where S is the set of indices of non-zero elements in \mathbf{d} that correspond to permanent ANs, and $\mathbf{a}_i = [x_i, y_i]^T$ is the known location of AN i .

Fig. 3 shows how the distance vector \mathbf{d} taken at point u in zone Z_1 of the apartment in Fig. 1 is processed. In Fig. 3, dots represent valid measured distances, while cross signs indicate missing values. At point u , the TN performed six successful ranging operations, i.e., four with permanent ANs and two with auxiliary ANs temporary placed into secondary APs 7 and 8. The complete distance vector \mathbf{d} is recorded in the distance database. The fingerprint for the zone database is obtained by applying the multilateration procedure on distance measurements to four permanent ANs. Note that because of NLOS paths between the TN and permanent ANs 3 and 4, the computed coarse position, \mathbf{c} , is only a rough estimate of the exact 2D coordinates of point u .

3.5. Online localization phase

During the online localization phase, only permanent ANs are in use, while all secondary APs are empty. The TN periodically initiates ranging rounds and sends an online distance vector to the location server after each round. The location server estimates the TN location by using fingerprint databases in order to improve localization accuracy.

The proposed online localization method is basically a trilateration procedure which is applied to the measured/estimated distances to three APs in the LOS-set of the zone where the target node is currently located. The distances for trilateration are obtained through two pre-processing steps, as illustrated in Fig. 4. In this figure, the online distance vector \mathbf{d} , comes from the TN located somewhere in the zone Z_1 of the apartment in Fig. 1. In the first step (zone identification), the zone database is used to identify the zone where the TN is currently in. In the second step (virtual distance measurement), the LOS-set associated with the identified zone is first retrieved from the configuration database, and then the distances to three APs in the LOS-set are determined. The distances to permanent ANs in the LOS-set are taken directly from the online distance vector, while the distances to secondary APs in the LOS-set are estimated by using the distance database. Finally, with known distances to three APs at disposal, the TN's location is calculated by a trilateration method.

3.5.1. Zone identification

To identify the zone, the TN's coarse position is first calculated by applying the least square-based multilateration algorithm to all non-zero distances in the online distance vector. Then, the TN's coarse position is classified into one of the zones by using well-known k -nearest neighbours (k NN) classification algorithm. With this algorithm, the zone is determined by majority voting, with the TN's coarse position being assigned to the zone most common among its k nearest neighbours in the zone database as measured by a distance function. For application in FAUL, we adopt $k = 3$ and Euclidean distance function:

$$\delta_{ZI}(\mathbf{c}_t, \mathbf{c}_f) = \sqrt{(x_t - x_f)^2 + (y_t - y_f)^2} \quad (3)$$

where $\mathbf{c}_t = (x_t, y_t)$, and $\mathbf{c}_f = (x_f, y_f)$ are coarse positions of TN and fingerprint in zone database, respectively. Note that the use of coarse positions solves the problem of missing values that could arise if the Euclidean distance function were applied directly to distance vectors with different subsets of zero-valued elements. Because of a limited range of UWB signal in indoor environments, the missing values, i.e. the zero-valued entries in distance vector, commonly appear. No matter which elements in the distance vector are missing, the coarse position can always be calculated as long as the number of non-zero elements is greater than or equal to three.

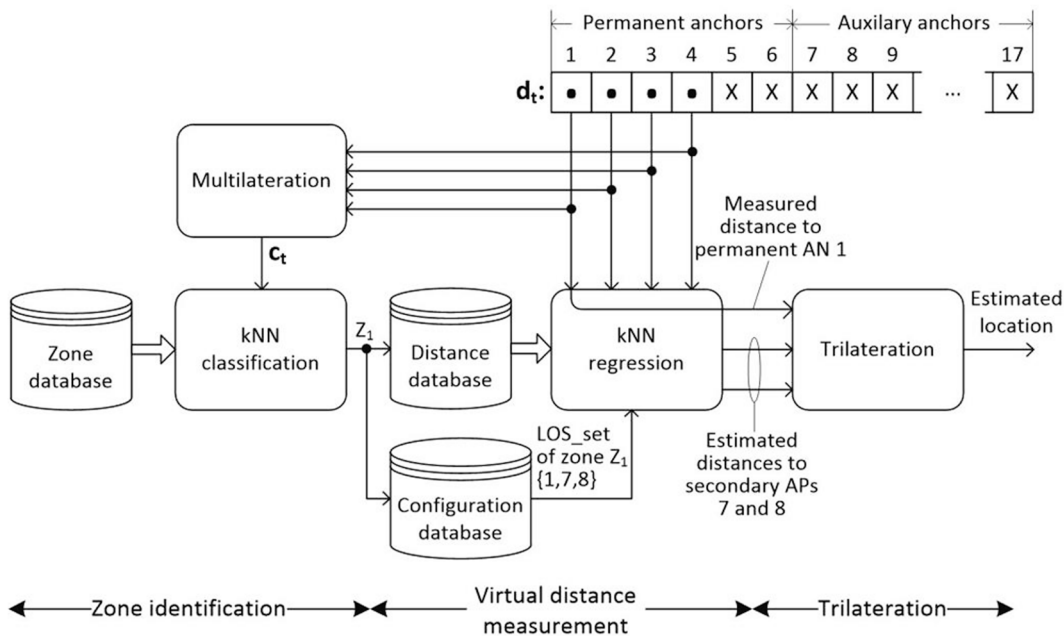


Fig. 4. Overview of the localization algorithm assuming that the online distance vector is taken in vicinity of point u in zone Z_1 of the apartment in Fig. 1.

3.5.2. Virtual distance measurement

Let the TN be located in zone Z_i with the LOS_set LS_i . If Z_i is p-PLOS covered, and $p = 3$, then this algorithm step is skipped, and the measured distances to three permanent ANs in LS_i are passed directly to the trilateration step. Otherwise, if $p < 3$, the $3-p$ missing distances for trilateration are determined through the process of *virtual distance-measurement* (VDM). Given online distance vector d_t , the VDM procedure estimates the most likely distances that would be measured by auxiliary ANs if they were placed in the corresponding secondary APs in LS_i . In FAUL, the VDM is implemented as a weighted kNN-based regression scheme that maps the online distance vector to the distances between TN and secondary APs in the LS_i . First, the algorithm finds k nearest neighbours comparing d_t and distance vectors of every fingerprint d_f in the distance database labeled with the zone Z_i . For comparison, we use the Euclidean distance function between d_t and d_f , by taking into account non-zero elements in both vectors, only:

$$\delta_{VDM}(d_t, d_f) = \sqrt{\sum_{i \in S}^N (d_t(i) - d_f(i))^2} \quad (4)$$

where S is the set of indices for which $d_t(i) \cdot d_f(i) \neq 0$. Note that d_t contains measured distances to primary ANs, only, while d_f additionally contains distances measured by auxiliary anchors placed into $p-3$ secondary APs from LS_i . After finding k nearest distance vectors in the distance database, the algorithm estimates the distance between TN and each secondary AP in LS_i as a weighted sum of elements that correspond to that AP in the selected neighboring distance vectors, adopting inverse of $\delta_{VDM}(d_t, d_f)$ as weights.

3.5.3. Trilateration

In the last step of the proposed online localization procedure, distances to three APs in the LOS-set of the identified zone are used to determine the 2D coordinates of the TN by applying a trilateration method. The accuracy of the trilateration method depends on the accuracy with which the three distances are measured/estimated. Obviously, the best localization accuracy can be obtained in 3-PLOS cases, where all three input distances for trilateration are the result of UWB ranging with permanent ANs under LOS conditions. On the other hand, localization under 0-PLOS conditions is the least accurate because of

unavoidable distance estimation errors induced by the VDM procedure. A common characteristic of these two boundary cases is that all three input distances have roughly the same contribution to the localization accuracy. This assumption clearly does not hold with 2-PLOS and 1-PLOS scenarios, where the less reliable VDM estimations are combined with highly accurate UWB measurements. As illustrated in Fig. 5(a), in 2-PLOS case, the TN is most probably located near one of two intersection points (u_1 and u_2) of two circles centered at the permanent ANs inserted in APs 1 and 3. However, the involvement of the third, less accurately estimated distance to secondary AP 2 in the trilateration process, with equal importance, could easily lead to displacement of the resulting position away from the exact position. Similarly, in the 1-PLOS case, the most probable location of the TN is a point on circle centered at the permanent AN (Fig. 5(b)). The presence of two less accurate distances could move the resulting location at the point that is further away or closer to the permanent AN than it is determined by the accurate UWB measurement.

To improve the localization accuracy in 1- and 2-PLOS cases, we adopt the weighted least-square trilateration method, which allows each input distance to be weighted based upon its type. The method gives higher weights to measured distances to permanent ANs, versus estimated distances to secondary APs. In particular, the weighted least-square algorithm finds the coordinates $\mathbf{u} = [x, y]^T$ of the TN that satisfy the following minimization problem:

$$\hat{\mathbf{u}} = [\hat{x}, \hat{y}]^T = \underset{x, y}{\operatorname{argmin}} \sum_{i=1}^3 w_i (\|\mathbf{a}_i - \mathbf{u}\| - d_i)^2 \quad (2)$$

where $\mathbf{a}_i = [x_i, y_i]^T$, $i = 1, 2, 3$ are coordinates of APs in the LOS-set, and d_i , $i = 1, 2, 3$ are measured/estimated distances to the corresponding APs. The weights w_i , $i = 1, 2, 3$ can take only two different values: w_p for primary, and w_s for secondary APs, where $w_p > w_s$. Note that in 3-PLOS and 0-PLOS cases, all three weights are of the same value, thus not affecting the trilateration result.

4. Results and discussion

This section presents an experimental evaluation of the proposed FAUL localization method. The evaluation was carried out within the experimental testbed platform deployed within $80m^2$ residential

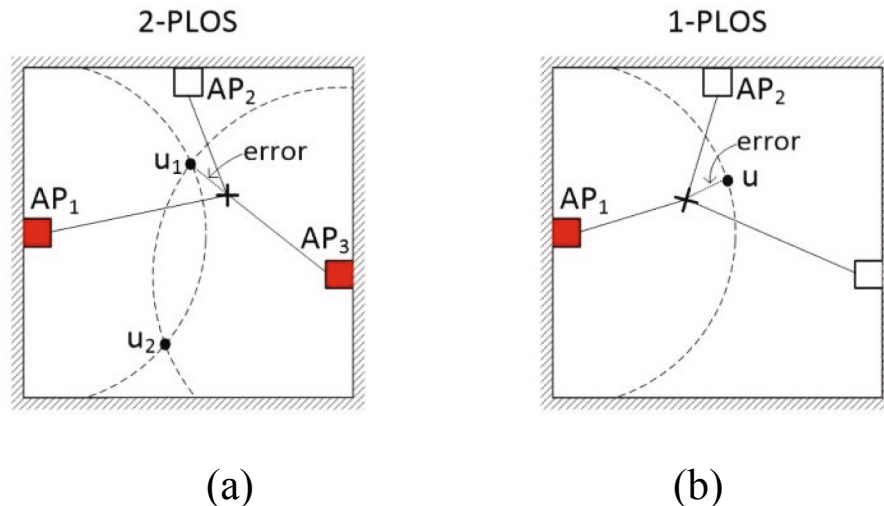


Fig. 5. Combining accurately measured distances to permanent anchors and estimated distances to secondary anchor placeholders can introduce significant localization error in: (a) 2-PLOS, and (b) 1-PLOS cases. Red boxes denote primary, while white boxes denote secondary anchor placeholders; cross signs denote estimated locations.

apartment whose layout is shown in Fig. 1. The apartment represents a typical complex indoor environment as it includes several rooms of different shapes and sizes. The testbed includes eight UWB nodes: seven ANs and one TN. The hardware design of UWB nodes is based on UWB compliant wireless transceiver DW1000 (DecaWave, 2018), which is used for both ranging and data communication. ANs are mounted on the walls at pre-specified positions 2m above the floor. The TN is attached to the top of a tripod 1m in height. We performed two sets of experiments to evaluate FAUL localization performances. In the first set of experiments, we examine how accurately FAUL identifies zones. The focus of the second set of experiments is FAUL coordinate-level accuracy.

4.1. Zone identification results

Accurate zone identification is of crucial importance for the FAUL's overall localization accuracy. With an incorrectly identified zone, a wrong LOS-set will be selected for the final localization, which may cause a considerable localization error. To estimate FAUL's zone-level accuracy, we collected distance vectors at a number of locations throughout the apartment at roughly every 20cm. During site-surveying, the user moved the tripod across the apartment briefly stopping for about 10 seconds at each location to allow the system to complete single ranging round, collect the measured distances, compute the coarse

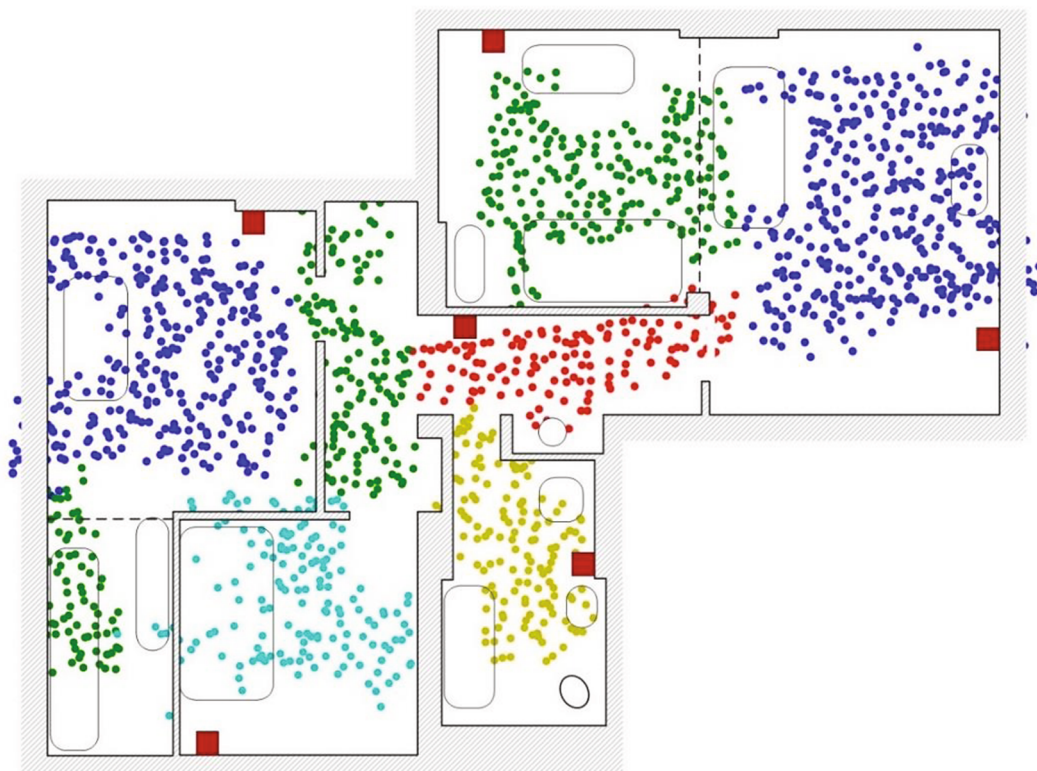


Fig. 6. Coarse positions of fingerprints in zone database.

position and store the fingerprint into the zone database. A total of 1.500 fingerprints are collected, with an average density of $25f/m^2$ (fingerprints per square meter).

Fig. 6 plots the coarse positions of all fingerprints in the zone database. The fingerprints taken in different zones are shown in different colours. The oval symbols on this map represent unmovable furniture. As can be noticed, the shape of each cluster of same-coloured dots only roughly matches the shape of the surveyed area within the corresponding zone. In some parts of the apartment, the dot clusters are skewed or squeezed, while in other parts are stretch and even cross the zone boundaries. These anomalies are expected since the coarse positions are calculated through the multilateration of all available TN-to-AN distances, most of which are measured under NLOS conditions. However, what is important to note is the minimal overlapping between neighbouring dot-clusters, which represents a prerequisite for accurate zone identification. Although NLOS propagation degrades coordinate-level accuracy, it actually useful in the context of zone identification. For example, propagation of the UWB signal through a typical $15cm$ wall increases the measured distance for about $15cm$ (Dardari, Conti, Ferner, Giorgetti, & Win, 2009), while reflections may add even a larger positive offset. The positive ranging offsets make fingerprints on opposite sides of a wall to appear further than they actually are, leading to a clear separation of fingerprint clusters from adjacent rooms.

In order to estimate FAUL's zone-level accuracy, we randomly select a fraction of the collected fingerprints for validation and leave the rest in the zone database. By varying the percent of the collected fingerprints selected for validation, we are able to investigate the influence of the fingerprint density on the zone-level accuracy. For each validation fingerprint, the zone is identified using the kNN classification algorithm with $k = 3$. The zone-level accuracy results are shown in Fig. 7. With a fingerprint density of $20f/m^2$, zone identification is correct 99.7% of the time. As expected, the zone-level accuracy decreases with the decrease of fingerprint density, but it is still above 90% even with the fingerprint density of only $1.25f/m^2$. These results point out that the UWB technology could be an effective solution for floor, room, and zone identification in complex indoor environments.

4.2. Localization results

The second experiment was carried out in a part of the zone Z_7 in room E of the apartment in Fig. 1 by collecting distance vectors at a grid of 20×36 reference points evenly spaced at $10cm$ apart, as depicted by grey dots in Fig. 8. The survey was carried out with ANs inserted into all three APs in the LOS set of zone Z_7 . At each grid point, ten ranging rounds were performed, each producing a distance vector containing eight non-zero distances: three to anchor nodes in the zone Z_7 (AP 6, 15, and 16) and remaining five to permanent ANs in other rooms (AP 1, ...,

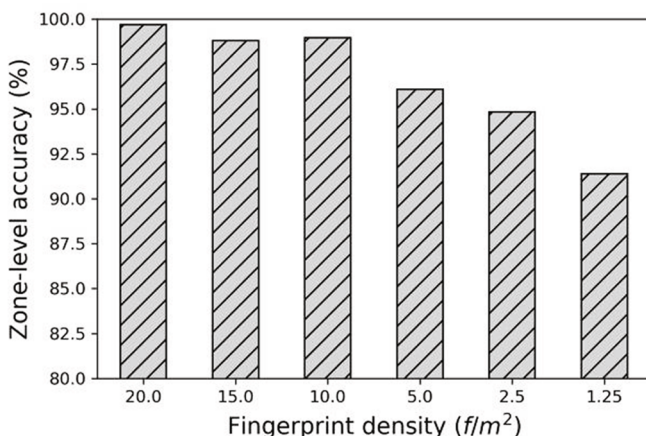


Fig. 7. Zone-level accuracy with varying fingerprint density.

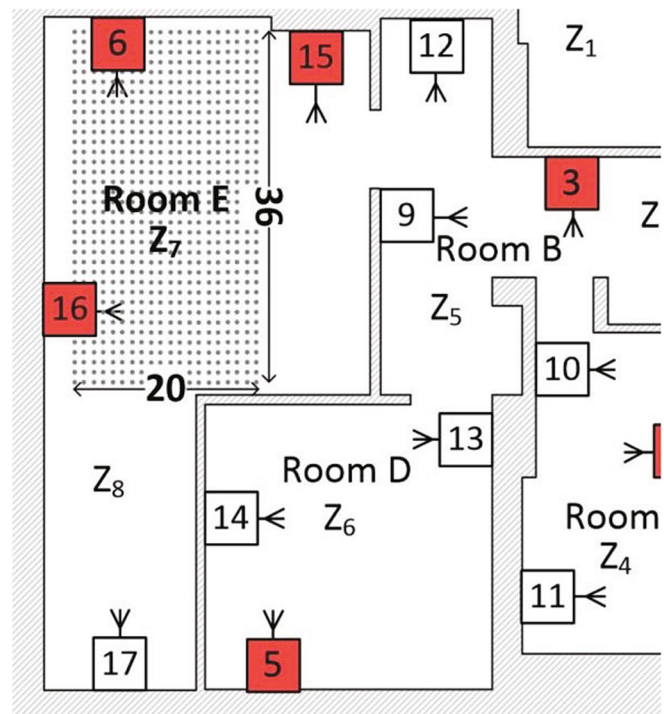


Fig. 8. Measurement grid points for localization accuracy test.

5). Fingerprint for distance database is generated by averaging distance vectors obtained in the first five ranging rounds. The remaining five distance vectors are also averaged and the resulting vector is saved into the test database that is used for validation. Ground truth coordinates of the grid points were manually measured with millimetre level of accuracy and also recorded. Note that the ground truth information is used only for the evaluation of ranging and localization errors, and is not supplied to FAUL.

We use measured data to analyse FAUL localization performances in four deployment scenarios: 3-, 2-, 1- and 0-PLOS. The content of the test database is used as a test case for 3-PLOS scenario. Test cases for the remaining three deployment scenarios are obtained by modifying the initial test database. To emulate the 2-PLOS scenario, we annul measured distances to AP 15 in all distance vectors in the test database. With this modification, before the trilateration step, FAUL will apply VDM to estimate the missing distance to AP 15. For the 1-PLOS test case, in addition to AP 15, distances to AP 16 are also annulled. Finally, the 0-PLOS test case is created by annulling measured distances to all three APs in zone Z_7 . We also tested FAUL performances under different fingerprint densities. We start the evaluation with the distance database containing the full set of 720 fingerprints, which corresponds to a fingerprint density of $100f/m^2$. We then repeated the evaluation using random subsets comprising 50%, 25%, 12.5%, and 6.25% of the full set.

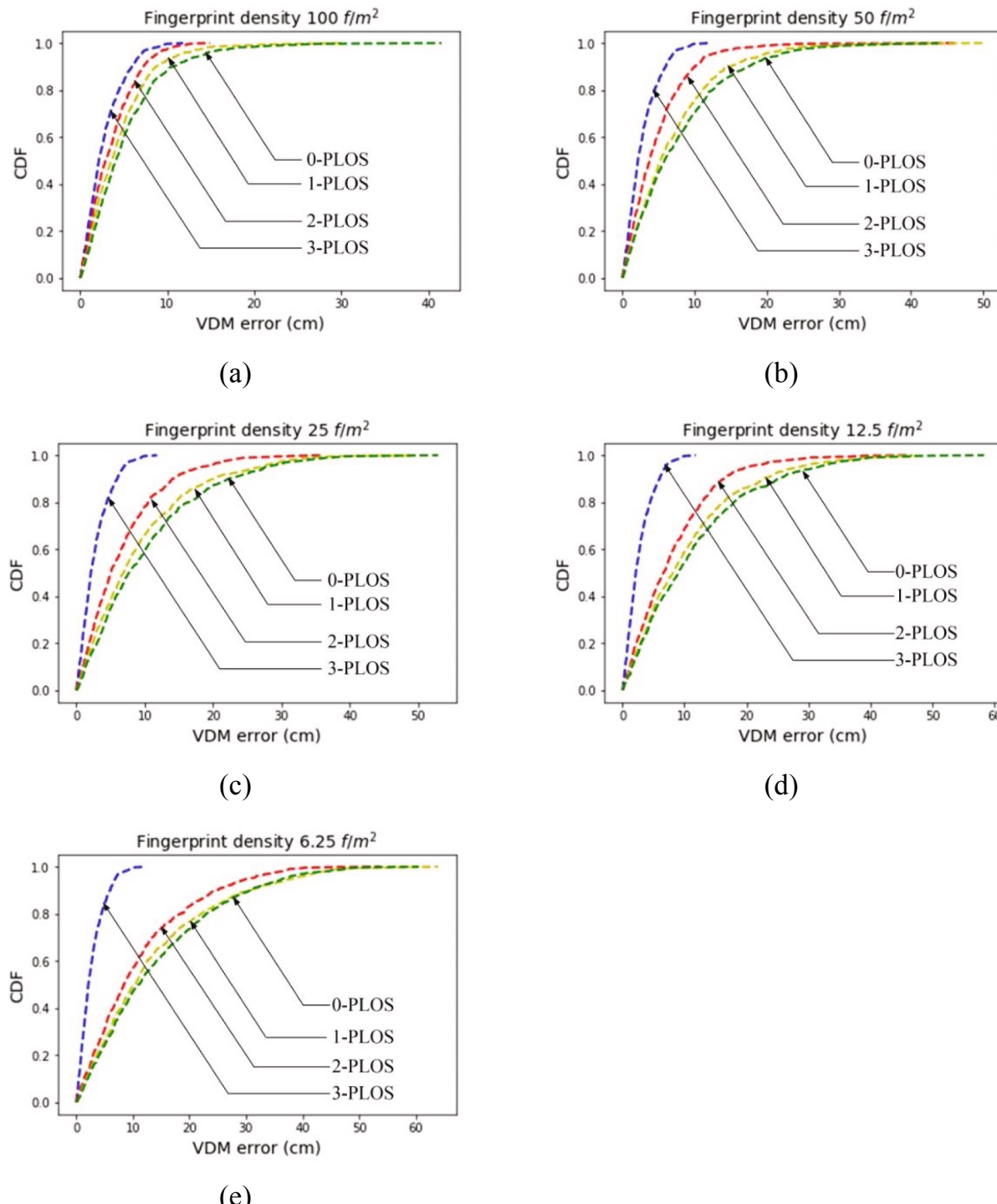
4.2.1. VDM accuracy

The first set of results corresponds to the accuracy of the VDM procedure. For each distance vector in the test database, VDM error, ε_{VDM} , was evaluated as the absolute difference between the actual distance from the corresponding grid point to the AP 6 and the distance to the same AP as estimated by VDM. The test is repeated for three deployment scenarios (2-, 1-, and 0-PLOS) and five fingerprint densities. The magnitude and uncertainty of VDM errors are quantified by Mean Distance Error (MDE), and Root Mean Square Error (RMSE) of ε_{VDM} . The results are reported in Table 1. The first row in this table corresponds to UWB ranging with AN inserted into AP 6 under LOS conditions. The obtained MDE and RMSE values of $2.8cm$ and $3.49cm$, respectively confirm high ranging accuracy and precision of DW1000 transceiver. As

Table 1

VDM error (in cm) for different number of LOS anchor nodes and fingerprint density.

Deployment scenario	Fingerprint density (f/m^2)									
	100		50		25		12.5		6.25	
	MDE	RMSE	MDE	RMSE	MDE	RMSE	MDE	RMSE	MDE	RMSE
UWB LOS	2.80/3.49									
VDM 2-PLOS	3.52	4.44	4.80	6.52	6.64	8.79	8.03	10.48	11.04	14.47
VDM 1-PLOS	4.42	5.85	7.00	9.46	9.07	12.15	10.32	13.64	13.45	17.74
VDM 0-PLOS	5.20	6.99	7.80	10.47	10.18	13.37	11.32	14.87	14.04	18.05

**Fig. 9.** CDF of the distance errors for VDM procedure when using distance database of density: a) $100 f/m^2$; b) $50 f/m^2$; c) $25 f/m^2$; d) $12.5 f/m^2$, and e) $6.25 f/m^2$.

can be noticed in [Table 1](#), at higher fingerprint densities, the estimation error of VDM is close to that of UWB LOS distance measurement. For example, while estimating the distance to AP 6 with two ANs inserted in APs 15 and 16 (2-PLOS case), and fingerprint density of $100f/m^2$, VDM introduces additional MDE of only $0.7cm$ compared with the direct UWB ranging. Even without ANs in zone Z_7 (0-PLOS case), the MDE of VDM is only $2.4cm$ larger than that of UWB ranging. As expected, the VDM accuracy decreases with the decrease of fingerprint density. As can be seen, under the 0-PLOS condition, a fingerprint density larger than $25f/m^2$ is required to keep the MDE of VDM smaller than $10cm$. However, with at least one AN in the zone Z_7 (1-PLOS case), a sub-decimetre average estimation error of VDM is obtained with fingerprint density of only $12.5f/m^2$.

[Fig. 9](#) shows the Cumulative Distribution Functions (CDFs) of ϵ_{VDM} for different fingerprint densities. The results indicate that for the fingerprint density of $100f/m^2$ VDM attains sub-decimetre accuracy in more than 80% of the cases in all deployment scenarios. However, when a relatively sparse distance database with a density of $12.5f/m^2$ is used, the VDM error is larger and ranges from more than $12cm$ (in the 2-PLOS scenario) to more than $20cm$ (in the 0-PLOS scenario) in 20% of the cases.

4.2.2. Coordinate-level accuracy

The second set of localization results illustrates the FAUL coordinate-level accuracy for different deployment scenarios and fingerprint densities. The coordinate-level accuracy is evaluated through the localization error, ϵ_{FAUL} , which is defined as the Euclidian distance between the actual position of a grid point and the position determined by the FAUL method. The weight parameters for the trilateration procedure are set to $w_p = 3$, and $w_s = 1$. [Table 2](#) reports the MDE and RMSE of ϵ_{FAUL} for 3-, 2-, 1-, and 0-PLOS deployment scenarios under different fingerprint densities. The distribution of the localization error is described by CDFs shown in [Fig. 10](#).

As expected, the best localization performances are attained in 3-PLOS scenario, where all three distances for trilateration are the result of accurate LOS UWB ranging. In particular, the MDE of $4.71cm$ is achieved, with ϵ_{FAUL} exceeding the localization error of $10cm$ in less than 5% of cases. In the remaining three deployment scenarios, FAUL relies on VDM to estimate distances to missing ANs, which inevitably increases the localization error. The accuracy of the final result depends on both the number of available LOS UWB-measured distances, and on how accurately VDM predicts the missing distances. It is important to observe that the localization accuracy in the 2-PLOS case is very close to that obtained in the 3-PLOS case, and only slightly drops with the decrease of the fingerprint density. The near-LOS accuracy in the 2-PLOS case is because of the adopted weighted trilateration method, in which LOS UWB-measured distances have a larger impact on the final location estimates than those obtained by VDM. In fact, in the 2-PLOS case, the only role of single VDM distance is the selection between two alternative locations determined by the remaining two LOS UWB-measured distances.

In the 1-PLOS case, single LOS UWB-measured distance cannot fully compensate for the lower accuracy of two VDM distances, which leads to increased localization error. With a high fingerprint density of $100f/m^2$,

the MDE is only $0.8cm$ larger than in the 3-PLOS case. However, when the distance database with a density of $6.25f/m^2$ is used for VDM estimations, FAUL produces localization error that is larger than $10cm$ in 50% of cases.

In the 0-PLOS deployment scenario, FAUL relies solely on VDM distances to determine the TN's location. Nevertheless, FAUL can attain relatively high coordinate-level accuracy even without LOS UWB-measured distances provided that the distance database of high fingerprint density is available. However, as the fingerprint density decreases, the localization error increases more rapidly than in the 1-PLOS scenario. For example, in the 0-PLOS case, the MDE with the fingerprint density of $25f/m^2$ is 1.94 times larger than with a density of $100fpm$. Under the same conditions, the MDE in the 1-PLOS case rises 1.57 times.

4.2.3. Impact of training data inaccuracy

In FAUL, the ground truth coordinates of grid points are not recorded during the offline fingerprint collection phase. Instead, the offline fingerprints include distances obtained by UWB ranging with auxiliary ANs that are temporarily placed into APs from the LOS set of the surveyed room. Thus, the fingerprint collection procedure can be performed automatically by the localization system, which greatly reduces the site-surveying effort. However, with this approach, UWB ranging errors are built in into the training data, which may lower the FAUL overall localization performance. To quantify the localization error induced by using auxiliary ANs during the offline phase, we repeat the coordinate-level accuracy analysis, but with the use of exact distances between grid points and auxiliary ANs instead of UWB measured distances.

[Table 3](#) shows the differences in MDE and RMSE (i.e., ΔMDE , and $\Delta RMSE$) of FAUL method when the distances to auxiliary ANs in offline location fingerprints are obtained by UWB ranging, and when the exact distances to auxiliary ANs are used. As expected, all ΔMDE and $\Delta RMSE$ values are positive, which indicates that the elimination of UWB ranging errors from training data improves the coordinate-level localization accuracy. However, the differences are rather small and do not exceed $2cm$ in all analysed deployment scenarios under different fingerprint densities. As can also be observed, the additional localization error due to the use of auxiliary ANs is larger with denser than with a sparse fingerprint database. At first glance, this observation may seem contradictory, but it can be explained by the fact that FAUL localization accuracy is influenced by both the accuracy of training data, and fingerprint density. When the fingerprint density is high, the UWB ranging inaccuracy represents the dominant source of localization errors. On the other hand, when a sparse fingerprint database is used, the removal of UWB ranging errors from training data cannot improve FAUL localization accuracy significantly, because of relatively larger localization error due to low fingerprint density.

4.2.4. Comparison with conventional fingerprinting approach

In order to gain insight into how the accuracy of FAUL is compared to the conventional kNN-based fingerprinting localization scheme (C-kNN), we applied the weighted kNN algorithm on the same test database that is used in the previous experiments. The C-kNN scheme requires that offline fingerprints be labelled with the ground truth coordinates. We analysed two C-kNN variants. In the first variant (C-kNN-E),

Table 2

Localization error (in cm) for different number of LOS anchor nodes and fingerprint densities.

Deployment scenario	Fingerprint density (f/m^2)									
	100		50		25		12.5		6.25	
	MDE	RMSE	MDE	RMSE	MDE	RMSE	MDE	RMSE	MDE	RMSE
3-PLOS	4.71/5.64									
2-PLOS	5.00	5.92	5.12	6.09	5.22	6.23	5.31	6.41	5.31	6.36
1-PLOS	5.74	6.78	7.18	9.71	9.04	11.16	10.3	12.74	12.8	15.87
0-PLOS	6.31	7.54	9.07	11.16	12.3	14.80	14.6	16.99	19.8	23.36

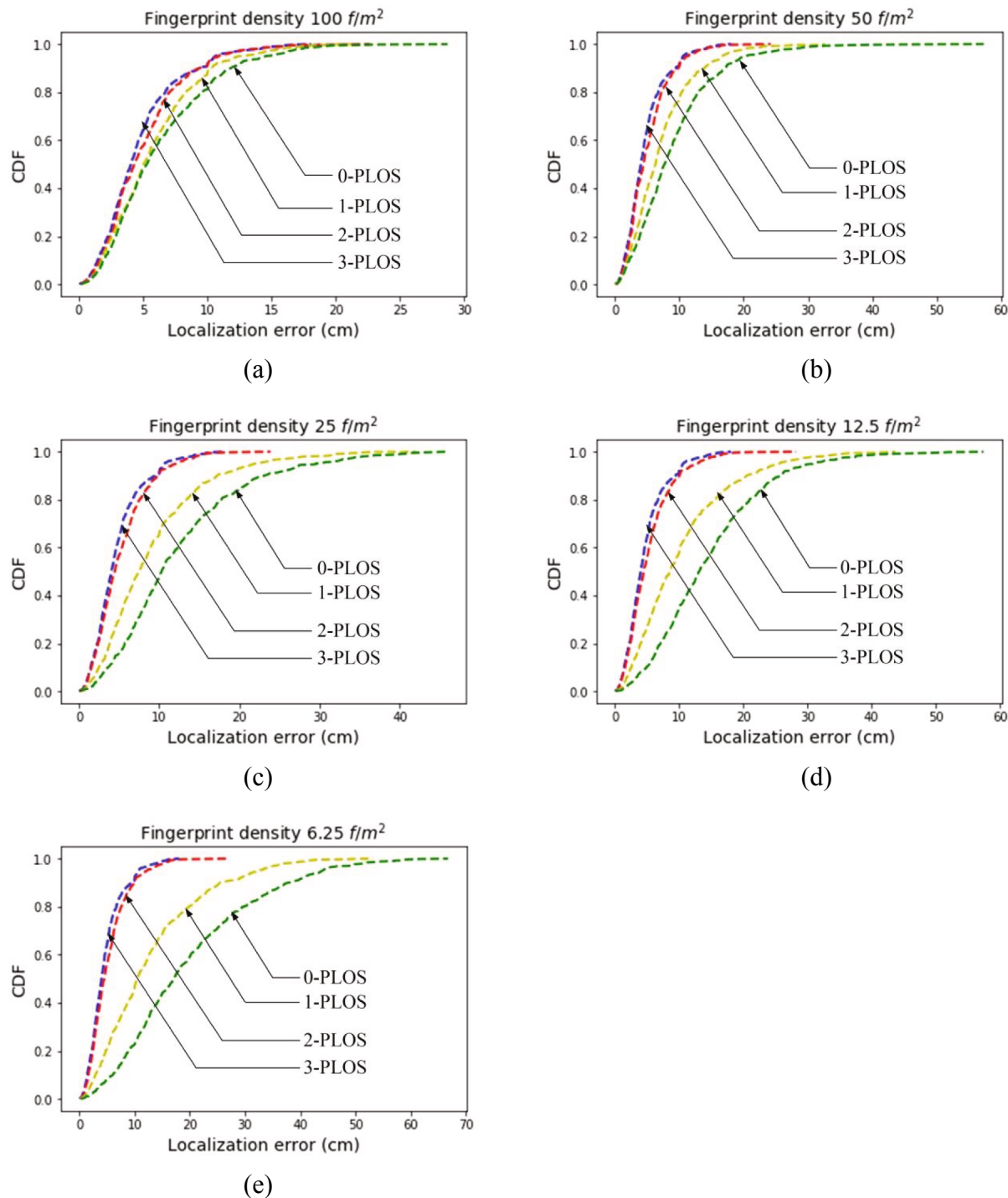


Fig. 10. CDF of localization errors for FAUL method when using distance database of density: a) $100\text{f}/\text{m}^2$; b) $50\text{f}/\text{m}^2$; c) $25\text{f}/\text{m}^2$; d) $12.5\text{f}/\text{m}^2$, and e) $6.25\text{f}/\text{m}^2$.

Table 3

Localization error (in cm) induced by using auxiliary ANs during fingerprint collection.

Deployment scenario	Fingerprint density (f/m^2)							
	100		50		25		12.5	
	ΔMDE	ΔRMSE	ΔMDE	ΔRMSE	ΔMDE	ΔRMSE	ΔMDE	ΔRMSE
3-PLOS	0/0							
2-PLOS	0.05	0.08	0.06	0.11	0.05	0.09	0.04	0.10
1-PLOS	0.95	1.06	0.77	1.83	0.62	0.74	0.38	0.44
0-PLOS	1.68	1.64	1.16	0.94	0.89	0.82	0.56	0.40

fingerprints are labelled with the exact ground truth locations, obtained by manually measuring coordinates of the grid points in the zone Z_7 (Fig. 8). In the second variant (C-kNN-A), the fingerprints are labelled with approximate estimations of grid point coordinates obtained by applying the trilateration algorithm to the UWB-measured distances to three LOS ANs in room E. In the online phase, both C-kNN algorithms compare the online fingerprint against those in the database and estimate the TN's location by averaging the ground truth coordinates of $k = 3$ most similar offline fingerprints.

Table 4 reports the coordinate-level accuracy results, in terms of MDE, for three competitive localization schemes. Note that the MDE data for the FAUL method are copied from Table 2. As we observe, despite using exact ground truth coordinates, C-kNN-E produces smaller localization errors than the FAUL method only if a very high-density fingerprint database is used. It should be noted that the manual construction of the fingerprint database with a density of $100f/m^2$ could take an enormous amount of time, even if the surveying area is relatively small. With the decrease of fingerprint density, the localization error of C-kNN schemes increases faster than that of FAUL. In the full LOS coverage scenario (3-PLOS), the localization error of C-kNN-E increase from $3.45cm$ to $12.04cm$ if the density of the fingerprint database is reduced from $100f/m^2$ to $12.5f/m^2$. As the FAUL method does not use the fingerprint database in the 3-PLOS scenario, its accuracy is not affected by fingerprint density. In the 2-PLOS scenario, the accuracy difference between FAUL and C-kNN-E follows a similar trend. The accuracy advantage of FAUL is also evident in the remaining two partially LOS coverage scenarios, although to a lesser extent. The performance advantage in a range of $1-2cm$ of C-kNN-E over C-kNN-A is due to approximate ground truth coordinates used in C-kNN-A. It is important to observe that the FAUL method achieves consistently lower localization error than C-kNN-A, including the fingerprint density of $100f/m^2$, even though both methods suffer for UWB ranging errors during the offline phase. This can be contributed to the fact that FAUL implements a more elaborate online localization algorithm, which favours LOS over NLOS measurements and uses the fingerprint database only when necessary to generate additional distances for trilateration.

4.3. Discussion

An important feature of the FAUL method is that the localization system can be partially reconfigured without interrupting the online operation. In particular, during the online phase, the user can insert one or more auxiliary ANs into a subset of secondary APs, or move auxiliary ANs from one to another subset of secondary APs, without the need to explicitly notify the location server about the changes. All distances measured between the TN and the auxiliary ANs will be present in the online distance vector at the positions reserved for corresponding secondary APs, and therefore they can be directly used for trilateration instead of VDM estimates. In this way, the user can easily extend the minimum system configuration (comprising permanent ANs, only) with additional ANs if there is a need to improve the localization accuracy in some critical parts of the environment. Another benefit of reconfiguration flexibility is the ability to seamlessly upgrade the distance database during the online phase. Instead of repeating the offline training, the

user can occasionally move auxiliary ANs from zone to zone during the online phase. Each time the location server receives a distance vector containing UWB-measured distances to all three APs in the LOS_set of the identified zone, it can create and insert a new fingerprint in the distance database by employing a suitable database updating scheme.

Although the FAUL is primarily intended for low-cost large-scale indoor deployments, it can also be adapted to other application scenarios. An interesting use case of FAUL is the high-accuracy fault-tolerant localization system, which relies on the full LOS coverage to achieve the maximum possible localization performance while providing the robustness against the AN failures. In this setup, the location server, as a background activity, continuously builds and updates the distance database with each distance vector received during the online operation. With three ANs deployed in every zone, the location system will not have to use the VDM procedure and distance database, as long as all ANs are operational. However, after any AN stops responding, either due to malfunctioning or depleted battery, the availability of the distance database will allow the location server to use the VDM procedure for estimating the missing distance. In this way, the localization system will be able to tolerate multiple faults with localization performance degrading gracefully as ANs fail, provided that each point in the localization space is still (LOS or NLOS) covered by at least three operational ANs.

5. Conclusions

In this paper, we have presented Fingerprint-Assisted UWB-based Localization (FAUL) method, a novel approach of improving the accuracy of the UWB localization system in complex indoor environments with a limited number of deployed anchors. FAUL combines fingerprinting and weighted trilateration techniques to reduce the localization error in situations when there are an insufficient number of line-of-sight (LOS) range measurements required for spatial localization. The key aspect of the proposed method is that the fingerprints are not labelled with their ground truth locations, as usual in most existing fingerprint-based approaches, but with distances to the set of pre-defined reference points distributed throughout the indoor environment. This localization approach favours LOS measurements and uses the fingerprinting database to predict distances to reference points only when necessary. Besides, FAUL considerably reduces the time and labour cost of building high-density fingerprint database during the offline training phase by using auxiliary anchors for distance measurement between the target node and the reference points. We have implemented FAUL in a typical five-room residential apartment intending to analyse the localization error in deployment scenarios when 3, 2, 1, and 0 LOS range measurements are available. Experiments show that FAUL attains approximately the same localization accuracy in the 2-PLOS case as in 3-PLOS case even with a low-density fingerprint database. In 1- and 0-LOS cases, the accuracy drops but it still can be maintained at sub-decimetre level, provided a fingerprint database of sufficient density (more than 50 fingerprints per meter squared) is available. One of our findings is that the UWB is very effective in room-identification, achieving the room-level localization accuracy of over 95% even with a relatively sparse fingerprint database. These results make FAUL an attractive approach for reducing system cost of UWB localization in indoor scenarios of

Table 4

Comparison of FAUL and conventional kNN-based fingerprinting scheme in terms of MDE (in cm) for different number of LOS ANs and fingerprint densities.

Deployment scenario	Fingerprint density (f/m^2)											
	100			50			25			12.5		
	FAUL	C-kNN-E	C-kNN-A	FAUL	C-kNN-E	C-kNN-A	FAUL	C-kNN-E	C-kNN-A	FAUL	C-kNN-E	C-kNN-A
3-PLOS	4.71	3.45	5.53	4.71	6.49	7.90	4.71	9.62	10.85	4.71	12.04	12.80
2-PLOS	5.00	4.05	6.06	5.12	7.54	8.83	5.22	11.02	12.04	5.31	13.62	14.30
1-PLOS	5.74	4.88	6.71	7.18	8.73	10.00	9.04	12.73	13.72	10.3	14.97	15.66
0-PLOS	6.31	6.49	8.05	9.07	11.14	12.24	12.3	15.33	16.20	14.6	18.38	19.06

complex geometry with an acceptable penalty in localization accuracy.

CRediT authorship contribution statement

Sandra Djosic: Conceptualization, Methodology, Software, Validation. **Igor Stojanovic:** Software, Data curation, Writing - original draft. **Milica Jovanovic:** Visualization, Investigation. **Tatjana Nikolic:** Validation, Investigation. **Goran Lj. Djordjevic:** Supervision, Writing - review & editing.

Declaration of Competing Interest

The authors declare that they have no known competing financial interests or personal relationships that could have appeared to influence the work reported in this paper.

Acknowledgment

This work was supported by Ministry of Education, Science and Technological Development of the Republic of Serbia.

References

- Alarifi, A., Al-Salman, A., Alsaleh, M., Alnafessah, A., Al-Hadrami, S., Al-Ammar, M. A., & Al-Khalifa, H. S. (2016). Ultra wideband indoor positioning technologies: Analysis and recent advances. *Sensors*, 16(5), 707. <https://doi.org/10.3390/s16050707>
- Bahl, P., & Padmanabhan, V. N. (2000). RADAR: An in-building RF-based user location and tracking system. In *Proceedings IEEE INFOCOM 2000. Conference on Computer Communications. Nineteenth Annual Joint Conference of the IEEE Computer and Communications Societies (Cat. No. 00CH37064)*, 2, 775–784. <https://doi.org/10.1109/INFCOM.2000.832252>
- Banitaan, S., Azzeh, M., & Nassif, A. B. (2016). User movement prediction: The contribution of machine learning techniques. In *2016 15th IEEE International Conference on Machine Learning and Applications (ICMLA)*, 571–575. <https://doi.org/10.1109/ICMLA.2016.0100>
- Belmonte-Fernandez, O., Montoliu, R., Torres-Sospedra, J., Sansano-Sansano, E., & Chia-Aguilar, D. (2018). A radiosity-based method to avoid calibration for indoor positioning systems. *Expert Systems With Applications*, 105, 89–101. <https://doi.org/10.1016/j.eswa.2018.03.054>
- Bergeron, F., Bouchard, K., Gaboury, S., & Giroux, S. (2018). Tracking objects within a smart home. *Expert Systems With Applications*, 113, 428–442. <https://doi.org/10.1016/j.eswa.2018.07.009>
- Bisio, I., Lavagetto, F., Marchese, M., & Sciarrone, A. (2013). Performance comparison of a probabilistic fingerprint-based indoor positioning system over different smartphones. In *2013 International Symposium on Performance Evaluation of Computer and Telecommunication Systems (SPECTS)*, 161–166.
- Bohdani, E., Vouyioukas, D., & Nomikos, N. (2016). Localization error modeling of hybrid fingerprint-based techniques for indoor ultra-wideband systems. *Telecommunication Systems*, 63(2), 223–241. <https://doi.org/10.1007/s11235-015-0116-4>
- Cai, Y., Rai, S. K., & Yu, H. (2015). Indoor positioning by distributed machine-learning based data analytics on smart gateway network. In *2015 International Conference on Indoor Positioning and Indoor Navigation (IPIN)*, 1–8. <https://doi.org/10.1109/IPIN.2015.7346934>
- Caso, G., Le, M. T., De Nardis, L., & Di Benedetto, M. G. (2018). Performance comparison of WiFi and UWB fingerprinting indoor positioning systems. *Technologies*, 6(1), 14. <https://doi.org/10.3390/technologies6010014>
- Chai, X., & Yang, Q. (2007). Reducing the calibration effort for probabilistic indoor location estimation. *IEEE Transactions on Mobile Computing*, 6(6), 649–662. <https://doi.org/10.1109/TMC.2007.1025>
- Chintalapudi, K., Padmanabha, I. A., & Padmanabhan, V. N. (2010). Indoor localization without the pain. In *Proceedings of the sixteenth annual international conference on Mobile computing and networking*, 173–184. <https://doi.org/10.1145/185995.1860016>
- DecaWave. DW1000 Module. (2018). <https://www.decawave.com/product/dwm1000-module/>.
- Dardari, D., Conti, A., Ferner, U., Giorgetti, A., & Win, M. Z. (2009). Ranging with ultrawide bandwidth signals in multipath environments. *Proceedings of the IEEE*, 97(2), 404–426. <https://doi.org/10.1109/JPROC.2008.2008846>
- Davidson, D., & Piché, R. (2016). A survey of selected indoor positioning methods for smartphones. *IEEE Communications Surveys & Tutorials*, 97(2), 404–426. <https://doi.org/10.1109/JPROC.2008.2008846>
- Farid, Z., Nordin, R., & Ismail, M. (2013). Recent advances in wireless indoor localization techniques and system. *Journal of Computer Networks and Communications*. <https://doi.org/10.1155/2013/185138>
- Ferreira, A. G., Fernandes, D., Catarino, A. P., & Monteiro, J. L. (2017). Performance analysis of ToA-based positioning algorithms for static and dynamic targets with low ranging measurements. *Sensors*, 17(8), 1915. <https://doi.org/10.3390/s17081915>
- Garcia, E., Poudereux, P., Hernandez, A., Urena, J., & Gualda, D. (2015). A robust UWB indoor positioning system for highly complex environments. *IEEE International Conference on Industrial Technology*, 3386–3391. <https://doi.org/10.1109/ICIT.2015.7125601>
- Gu, Y., Lo, A., & Niemegeers, I. (2009). A survey of indoor positioning systems for wireless personal networks. *IEEE Communications Surveys & Tutorials*, 11(1), 13–32. <https://doi.org/10.1109/SURV.2009.090103>
- Gururaj, K., Rajendra, A. K., Song, Y., Law, C. L., & Cai, G. (2017). Real-time identification of NLOS range measurements for enhanced UWB localization. *International Conference on Indoor Positioning and Indoor Navigation*, 1–7. <https://doi.org/10.1109/IPIN.2017.8115877>
- Guvenc, I., Chong, C. C., & Watanabe, F. (2007). NLOS identification and mitigation for UWB localization systems. In *2007 IEEE Wireless Communications and Networking Conference*, 1571–1576. <https://doi.org/10.1109/WCNC.2007.296>
- Güvenç, I., Chong, C. C., Watanabe, F., & Inamura, H. (2007). NLOS identification and weighted least-squares localization for UWB systems using multipath channel statistics. *EURASIP Journal on Advances in Signal Processing*, 2008, 1–14. <https://doi.org/10.1155/2008/271984>
- He, S., & Chan, S. H. G. (2015). Wi-Fi fingerprint-based indoor positioning: Recent advances and comparisons. *IEEE Communications Surveys & Tutorials*, 18(1), 466–490. <https://doi.org/10.1109/COMST.2015.2464084>
- Huang, K., He, K., & Du, X. (2019). A hybrid method to improve the BLE-based indoor positioning in a dense Bluetooth environment. *Sensors*, 19(2), 424. <https://doi.org/10.3390/s19020424>
- Kaemarungsi, K., & Krishnamurthy, P. (2012). Analysis of WLAN's received signal strength indication for indoor location fingerprinting. *Pervasive and Mobile Computing*, 8(2), 292–316. <https://doi.org/10.1016/j.pmcj.2011.09.003>
- Khodjaev, J., Park, Y., & Malik, A. S. (2010). Survey of NLOS identification and error mitigation problems in UWB-based positioning algorithms for dense environments. *Annals of Telecommunications-Annales des Télécommunications*, 65(5–6), 301–311. <https://doi.org/10.1007/s12243-009-0124-z>
- Liu, H., Darabi, H., Banerjee, P., & Liu, J. (2007). Survey of wireless indoor positioning techniques and systems. *IEEE Transactions on Systems, Man, and Cybernetics, Part C (Applications and Reviews)*, 37(6), 1067–1080. <https://doi.org/10.1109/TSMCC.2007.905750>
- Luo, J., & Gao, H. (2016). Deep belief networks for fingerprinting indoor localization using ultrawideband technology. *International Journal of Distributed Sensor Networks*, 12(1), 5840916. <https://doi.org/10.1155/2016/5840916>
- Neirynck, D., Luk, E., & McLaughlin, M. (2016). An alternative double-sided two-way ranging method. In *2016 13th workshop on positioning, navigation and communications (WPNC)*, 1–4. <https://doi.org/10.1109/WPNC.2016.7822844>
- Prorok, A., & Martinoli, A. (2014). Accurate indoor localization with ultra-wideband using spatial models and collaboration. *The International Journal of Robotics Research*, 33(4), 547–568. <https://doi.org/10.1177/0278364913500364>
- Ruiz, A. R. J., & Granja, F. S. (2017). Comparing ubisense, bespoon, and decawave uwb location systems: Indoor performance analysis. *IEEE Transactions on instrumentation and Measurement*, 66(8), 2106–2117. <https://doi.org/10.1109/TIM.2017.2681398>
- Sciarrone, A., Fiandrino, C., Bisio, I., Lavagetto, F., Kliazovich, D., & Bouvry, P. (2016). Smart probabilistic fingerprinting for indoor localization over fog computing platforms. In *2016 5th IEEE International Conference on Cloud Networking (CloudNet)*, 39–44. <https://doi.org/10.1109/CloudNet.2016.433>
- Song, B., Zhang, S., Long, J., & Hu, Q. (2017). Fingerprinting localization method based on toa and particle filtering for mines. *Mathematical Problems in Engineering*. <https://doi.org/10.1155/2017/3215978>
- Steiner, C., & Wittneben, A. (2009). Low complexity location fingerprinting with generalized UWB energy detection receivers. *IEEE Transactions on Signal Processing*, 58(3), 1756–1767. <https://doi.org/10.1109/TSP.2009.2036060>
- Stella, M., Russo, M., & Begušić, D. (2014). Fingerprinting based localization in heterogeneous wireless networks. *Expert systems with Applications*, 41(15), 6738–6747. <https://doi.org/10.1016/j.eswa.2014.05.016>
- Talvitie, J., Renfors, M., & Lohan, E. S. (2015). Distance-based interpolation and extrapolation methods for RSS-based localization with indoor wireless signals. *IEEE Transactions on Vehicular Technology*, 64(4), 1340–1353. <https://doi.org/10.1109/TVT.2015.2397598>
- Tiemann, J., Schweikowski, F., & Wietfeld, C. (2015). Design of an UWB indoor-positioning system for UAV navigation in GNSS-denied environments. In *2015 International Conference on Indoor Positioning and Indoor Navigation (IPIN)*, 1–7. <https://doi.org/10.1109/IPIN.2015.7346960>
- Velimirović, A. S., Djordjević, G. L., Velimirović, M. M., & Jovanović, M. D. (2012). Fuzzy ring-overlapping range-free (FRORF) localization method for wireless sensor networks. *Computer Communications*, 35(13), 1590–1600. <https://doi.org/10.1016/j.comcom.2012.05.006>
- Yan, J., Tiberius, C. C., Janssen, G. J., Teunissen, P. J., & Bellusci, G. (2013). Review of range-based positioning algorithms. *IEEE Aerospace and Electronic Systems Magazine*, 28(8), 2–27. <https://doi.org/10.1109/MAES.2013.6575420>
- Yang, Z., Wu, C., & Liu, Y. (2012). Locating in fingerprint space: wireless indoor localization with little human intervention. In *Proceedings of the 18th annual international conference on Mobile computing and networking*, 269–280. <https://doi.org/10.1145/2348543.2348578>
- You, B., Li, X., Zhao, X., & Gao, Y. (2015). A novel robust algorithm attenuating non-line-of-sight errors in indoor localization. In *2015 IEEE International Conference on Communication Software and Networks (ICCSN)*, 6–11. <https://doi.org/10.1109/ICCSN.2015.7296117>
- Yu, L., Laaraiedh, M., Avrillon, S., & Uguen, B. (2011). Fingerprinting localization based on neural networks and ultra-wideband signals. In *2011 IEEE international symposium*

- on signal processing and information technology (ISSPIT), 184–189. <https://doi.org/10.1109/ISSPIT.2011.6151557>
- Zafari, F., Gkelias, A., & Leung, K. K. (2019). A survey of indoor localization systems and technologies. *IEEE Communications Surveys & Tutorials*, 21(3), 2568–2599. <https://doi.org/10.1109/COMST.2019.2911558>
- Zhang, J., Orlik, P. V., Sahinoglu, Z., Molisch, A. F., & Kinney, P. (2009). UWB systems for wireless sensor networks. *Proceedings of the IEEE*, 97(2), 313–331. <https://doi.org/10.1109/JPROC.2008.2008786>
- Zhao, F., Huang, T., & Wang, D. (2019). A Probabilistic Approach for WiFi Fingerprint Localization in Severely Dynamic Indoor Environments. *IEEE Access*, 7, 116348–116357. <https://doi.org/10.1109/ACCESS.2019.2935225>
- Zwirello, L., Schipper, T., Jalilvand, M., & Zwick, T. (2014). Realization limits of impulse-based localization system for large-scale indoor applications. *IEEE Transactions on Instrumentation and Measurement*, 64(1), 39–51. <https://doi.org/10.1109/TIM.2014.2332241>